Research Article

István Ecsedi and Ákos József Lengyel*

Deformation of rotating two-layer curved composite beams

https://doi.org/10.1515/cls-2019-0015
Received Jun 17, 2019; accepted Aug 16, 2019

Abstract: An analytical solution is presented for the determination of the deformation of rotating two-layer composite beams. The direction of axis of rotation is vertical and the speed of rotation is constant. The axis of rotation is in the plane of symmetry of curved beam. The source of the in-plane deformation is the stationary rotation of the curved beam. The plane of the curvature is the symmetry plane of the curved beam for its material, geometrical and supporting properties. Assumed form of the displacement field meets the prescriptions of the classical Euler-Bernoulli beam theory. Examples illustrate the applications of the presented analytical solution.

Keywords: Analytical solution; two-layer curved beam; in-plane deformation

1 Introduction

Rotating curved beams are basic units in many structures and industrial applications. Nowadays the analysis of curved composite beams is an important topic in the structural mechanics. For the solution of static bending problems of layered curved beam Segura and Armengaud gave an analytical method [1]. Elasticity solutions are presented in [2] for curved beams with orthotropic functionally graded layers by means of Airy stress function. The developed method is illustrated in curved cantilever beams with different types of loading conditions. Paper by Pydah and Sabale [3] presents an analytical model for the flexure of bidirectional functionally graded circular beams based on the Euler-Bernoulli beam theory. The material properties are simultaneously smooth function of the radial coordinate r and the polar angle φ. The governing equations are solved for statically determinate circular cantilever beams under the action of tip load.

It must be mentioned that papers by Ecsedi and Lengyel [4, 5] provide analytical solutions for layered curved composite beams with interlayer slip. In paper [4] the deformation of curved composite beams with partial shear interaction is determined under the action of concentrated radial load. Paper [5] gives numerical solution for in-plane deformation of two-layer composite beam with flexible shear connection by application of the principle of minimum of potential energy. An analytical solution is presented in [6] for the static problems of curved composite beams. The analytical solution formulated by Ecsedi and Lengyel is based on fundamental solutions. Linear combination of the fundamental solutions which satisfy the given loading and boundary conditions gives the solution of considered static boundary value problem [6].

Static problems of curved composite beams were analysed by finite element methods in papers of Ibrahimbegović and Frey [7], Ascione and Fraternali [8], Bhimaraddi [9], Dorfi and Busby [10], Kim [11]. There exist several works on the solution of static problems of curved composite beams, it is not the aim of this paper to give a complete list of the above mentioned papers.

It should be mentioned that several papers deal with the vibration analysis of rotating curved beams. In these papers the axis of rotation is perpendicular to the plane of circular centre line and the main goal is to determine the eigenfrequencies of free vibrations. In paper by Wang and Mahrenholtz [13] the bending vibration of rotating curved beam is investigated by using Galerkin's method. Longitudinal and Coriolis effects are neglected. Park and Kim deal with the dynamic properties of curved beam [14]. The derived equations of motion in [14] include the Coriolis and centrifugal forces, linear and non-linear FEM formulations are developed and the effects of curvature and tip mass to the motion are also studied in [14]. Paper by Chen et al. [15] presents a dynamic model of rotating curved beam which is based on the Absolute Nodal Coordinate Formulation and on the radial integration method. Chidamparam and Leissa [16] gives a detailed analysis on the vibration

István Ecsedi: Institute of Applied Mechanics, University of Miskolc, Miskolc-Egyetemváros, H-3515 Miskolc, Hungary; Email: mechecs@uni-miskolc.hu
***Corresponding Author: Ákos József Lengyel:** Institute of Applied Mechanics, University of Miskolc, Miskolc-Egyetemváros, H-3515 Miskolc, Hungary; Email: mechlen@uni-miskolc.hu

of curved beams, rings which lie in plane. In-plane, out-of-plane and coupled vibrations are considered in [16]. Kartav in [17] is studied the free vibration problem of rotating curved beams with variable cross section by the use of Finite Difference Method and Finite Element Method.

In the present paper an analytical solution is formulated for rotating two-layer composite curved beams. The connection of curved beam components is perfect and the plane of curvature is the symmetry plane for the geometrical, material properties and loading conditions. In-plane deformations are considered and the speed of rotation of curved beams is uniform. The source of the deformation is the system of centrifugal forces. Figure 1 shows the rotating curved two-layer composite beam. In the cylindrical coordinate system $Or\varphi z$ the curved layer B_i ($i = 1, 2$) occupies the space domain

$$B_i = \left\{(r, \varphi, z) | (r, z) \in A_i, \quad \varphi_1 \le \varphi \le \varphi_2 \le 2\pi, \ |z| \le \frac{t}{2}\right\}, \quad (i = 1, 2), \tag{1}$$

where A_i is the cross section of beam component i ($i = 1, 2$) (Figure 1). The common boundary of B_1 and B_2 is denoted by ∂B_{12}

$$\partial B_{12} = \left\{(r, \varphi, z) | r = c, \ \varphi_1 \le \varphi_2 \le 2\pi, \ |z| \le \frac{t}{2}\right\}. \tag{2}$$

In Eq. (2) t denotes the thickness of the rectangular cross sections A_1 and A_2 (Figure 1). The formulation of the analytical solution developed in this paper is based on [12]. Paper [12] presents a simple one-dimensional mechanical model to analyse the static and dynamic features of non-homogeneous curved beam. The model of paper [12] is based on the Euler-Bernoulli beam theory. The rotary inertia is included in the expression of system of centrifugal forces.

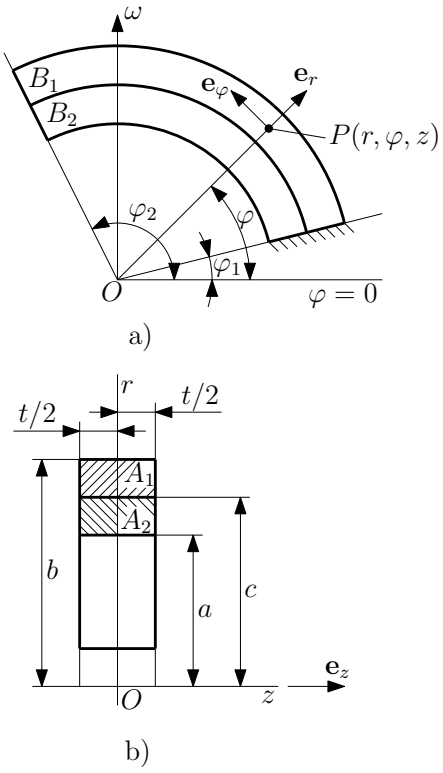

Figure 1: Rotating two-layer curved beam (a) and its cross section (b).

2 Governing equation

The in-plane deformation of rotating curved two-layer composite beam is described by the next displacement field in the cylindrical coordinate system $Or\varphi z$ [12]

$$\mathbf{u} = u\mathbf{e}_r + v\mathbf{e}_\varphi + w\mathbf{e}_z, \tag{3}$$

$$u = U(\varphi), \quad v = r\phi(\varphi) + \frac{\mathrm{d}U}{\mathrm{d}\varphi}, \quad w = 0. \tag{4}$$

In Eq. (3) $\mathbf{e}_r$, $\mathbf{e}_\varphi$ and $\mathbf{e}_z$ are the unit vectors of the cylindrical coordinate system $Or\varphi z$ (Figure 1). From the strain-displacement relationships of the linearised theory of elasticity we obtain

$$\varepsilon_r = \frac{\partial u}{\partial r} = 0, \quad \varepsilon_z = \frac{\partial w}{\partial z} = 0, \quad \gamma_{rz} = \frac{\partial u}{\partial z} + \frac{\partial w}{\partial r} = 0, \tag{5}$$

$$\gamma_{\varphi z} = \frac{1}{r}\frac{\partial w}{\partial \varphi} + \frac{\partial v}{\partial z} = 0, \quad \gamma_{r\varphi} = \frac{\partial v}{\partial r} - \frac{v}{r} + \frac{1}{r}\frac{\partial u}{\partial \varphi} = 0. \tag{6}$$

$$\varepsilon_\varphi = \frac{u}{r} + \frac{1}{r}\frac{\partial v}{\partial \varphi} = \frac{1}{r}\left(U + \frac{\mathrm{d}^2 U}{\mathrm{d}\varphi^2}\right) + \frac{\mathrm{d}\phi}{\mathrm{d}\varphi}. \tag{7}$$

In Eqs. (5–7), ε_r, ε_φ, ε_z are the normal strains and $\gamma_{r\varphi}$, γ_{rz}, $\gamma_{\varphi z}$ are the shearing strains. Application of the Hooke's law gives

$$\sigma_\varphi = E(r, z)\left\{\frac{1}{r}\left(U + \frac{\mathrm{d}^2 U}{\mathrm{d}\varphi^2}\right) + \frac{\mathrm{d}\phi}{\mathrm{d}\varphi}\right\}. \tag{8}$$

In Eq. (8) σ_φ is the normal stress and other stress components are equal to zero, furthermore $E = E(r, z)$ is the modulus of elasticity which may depend on the cross-sectional coordinate r and z. Following the formulation presented in paper [12] we introduce the next cross-sectional and material properties (Figure 1)

$$AE_0 = E_1A_1 + E_2A_2, \quad A = A_1 + A_2, \tag{9}$$

$$\frac{AE_0}{R} = \frac{E_1A_1}{R_1} + \frac{E_2A_2}{R_2}, \tag{10}$$

$$\frac{1}{R_1} = \frac{\ln\frac{b}{c}}{b-c}, \quad \frac{1}{R_2} = \frac{\ln\frac{c}{a}}{c-a}, \tag{11}$$

$$r_c = \frac{\int\limits_A rE(r,z)\mathrm{d}A}{AE_0} = \frac{E_1r_1(b-c) + E_2r_2(c-a)}{b-a}, \tag{12}$$

$$r_1 = \frac{c+b}{2}, \quad r_2 = \frac{a+c}{2}, \quad e = r_c - R, \tag{13}$$

$$q_1 = \rho_1 t \int\limits_c^b r^2\mathrm{d}r = \rho_1\frac{t}{3}\left(b^3 - c^3\right), \tag{14}$$

$$q_2 = \rho_2 t \int\limits_a^c r^2\mathrm{d}r = \rho_2\frac{t}{3}\left(c^3 - a^3\right), \tag{15}$$

$$Q_1 = \rho_1 t \int\limits_c^b r^3\mathrm{d}r = \rho_1\frac{t}{4}\left(b^4 - c^4\right), \tag{16}$$

$$Q_2 = \rho_2 t \int\limits_a^c r^3\mathrm{d}r = \rho_2\frac{t}{4}\left(c^4 - a^4\right), \tag{17}$$

$$q = q_1 + q_2, \quad Q = Q_1 + Q_2, \tag{18}$$

where E_i is the modulus of elasticity of layer i and ρ_i is the mass density of layer i ($i = 1, 2$). In order to formulate the equations of mechanical equilibrium we define the next stress resultants-displacements relationships according to paper [12] as

$$N(\varphi) = \int\limits_A \sigma_\varphi\mathrm{d}A = AE_0\left[\frac{1}{R}\left(U + \frac{\mathrm{d}^2U}{\mathrm{d}\varphi^2}\right) + \frac{\mathrm{d}\phi}{\mathrm{d}\varphi}\right], \tag{19}$$

$$M(\varphi) = \int\limits_A r\sigma_\varphi\mathrm{d}A = AE_0\left[U + \frac{\mathrm{d}^2U}{\mathrm{d}\varphi^2} + r_c\frac{\mathrm{d}\phi}{\mathrm{d}\varphi}\right], \tag{20}$$

$$S(\varphi) = \int\limits_A \tau_{r\varphi}\mathrm{d}A. \tag{21}$$

In Eq. (21) $\tau_{r\varphi}$ is the shearing stress. The equation of mechanical equilibrium in terms of N, S and M can be formulated as

$$\frac{\mathrm{d}N}{\mathrm{d}\varphi} + S + f_\varphi = 0, \tag{22}$$

$$-N + \frac{\mathrm{d}S}{\mathrm{d}\varphi} + f_r = 0, \tag{23}$$

$$\frac{\mathrm{d}M}{\mathrm{d}\varphi} + m = 0. \tag{24}$$

In Eqs. (22–24) f_r, f_φ and m are the applied forces and moment, respectively. The dimension of f_r and f_φ is [force] and the dimension of m is [force×length]. From Eq. (21) and Eq. (23) it follows that

$$S(\varphi) = -AE_0\left[\frac{1}{R}\left(\frac{\mathrm{d}^3U}{\mathrm{d}\varphi^3} + \frac{\mathrm{d}U}{\mathrm{d}\varphi}\right) + \frac{\mathrm{d}^2\phi}{\mathrm{d}\varphi^2}\right] - f_\varphi. \tag{25}$$

Elimination of shear force $S(\varphi)$ from Eqs. (22) and (23) leads to the equation

$$\frac{\mathrm{d}^2N}{\mathrm{d}\varphi^2} + N + \frac{\mathrm{d}f_\varphi}{\mathrm{d}\varphi} - f_r = 0. \tag{26}$$

3 Determination of system of centrifugal forces

Figure 2 shows a volume element of curved beam $\mathrm{d}B = tr\mathrm{d}r\mathrm{d}\varphi$ which loaded by centrifugal force $\mathrm{d}f$. It is evident

$$\mathrm{d}f = \omega^2\rho(r)tr^2\cos\varphi\mathrm{d}r\mathrm{d}\varphi. \tag{27}$$

We define the centrifugal force element $\mathrm{d}f_1$ which acts on the volume element determined by cylindrical surfaces given by $r = c$ and $r = b$ and two planes given by φ and $\mathrm{d}\varphi$

$$\mathrm{d}f_1 = \omega^2 q_1\cos\varphi\mathrm{d}\varphi. \tag{28}$$

The centrifugal force element $\mathrm{d}f_2$ acts on the volume element determined by cylindrical surfaces $r = a$ and $r = c$ and two planes which are given by φ and $\varphi + \mathrm{d}\varphi$

$$\mathrm{d}f_2 = \omega^2 q_2\cos\varphi\mathrm{d}\varphi. \tag{29}$$

The total centrifugal force element is

$$\mathrm{d}f_c = \mathrm{d}f_1 + \mathrm{d}f_2 = \omega^2 q\cos\varphi\mathrm{d}\varphi. \tag{30}$$

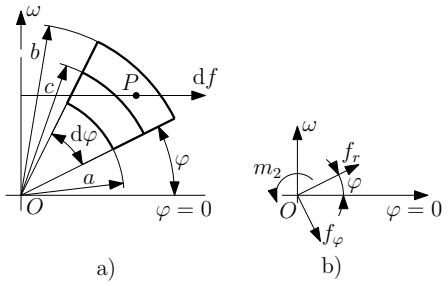

Figure 2: Determination of system of centrifugal forces.

It is evident that $\mathrm{d}f_c$ can be replaced by an equivalent force couple at the origin O of cylindrical coordinate system $Or\varphi z$ [12] (Figure 2b)

$$f_r \mathrm{d}\varphi = \omega^2 q \cos^2\varphi \mathrm{d}\varphi, \quad f_\varphi \mathrm{d}\varphi = -\omega^2 \frac{q}{2} \sin 2\varphi \mathrm{d}\varphi, \quad (31)$$

$$m_z \mathrm{d}\varphi = -\frac{\omega^2}{2} Q \sin 2\varphi \mathrm{d}\varphi. \quad (32)$$

The deformation of the curved two-layer composite beam is obtained from the system of equilibrium equations

$$\frac{\mathrm{d}^2 N}{\mathrm{d}\varphi^2} + N - 3\omega^2 q \cos^2\varphi + \omega^2 q = 0, \quad (33)$$

$$\frac{\mathrm{d}M}{\mathrm{d}\varphi} - \frac{\omega^2}{2} Q \sin 2\varphi = 0. \quad (34)$$

We reformulate Eq. (33) as

$$-\frac{\mathrm{d}^2 N}{\mathrm{d}\varphi^2} + N - \frac{3}{2}\omega^2 q \cos 2\varphi - \frac{1}{2}\omega^2 q = 0. \quad (35)$$

4 Determination of radial displacement and cross-sectional rotation

The combination of Eq. (19) with (35) and Eq. (20) with Eq. (34) provide

$$AE_0 \left[\frac{\mathrm{d}^2 W}{\mathrm{d}\varphi^2} + W + R\left(\frac{\mathrm{d}^3\phi}{\mathrm{d}\varphi^3} + \frac{\mathrm{d}\phi}{\mathrm{d}\varphi}\right)\right] = \frac{\omega^2}{2} Rq + \frac{3}{2}\omega^2 Rq \cos 2\varphi, \quad (36)$$

$$AE_0 \left(\frac{\mathrm{d}W}{\mathrm{d}\varphi} + r_c \frac{\mathrm{d}^2\phi}{\mathrm{d}\varphi^2}\right) = \frac{\omega^2}{2} Q \sin 2\varphi, \quad (37)$$

here

$$W(\varphi) = U + \frac{\mathrm{d}^2 U}{\mathrm{d}\varphi^2}. \quad (38)$$

The solution of the system of differential equations (36), (37) for $W = W(\varphi)$ and $\phi = \phi(\varphi)$ is as follows

$$W(\varphi) = \frac{\omega^2}{2AE_0} Rq + C_w \cos 2\varphi + r_c C_2 \sin\varphi - r_c C_3 \cos\varphi, \quad (39)$$

$$\phi(\varphi) = C_\phi \sin 2\varphi + C_0 + C_1\varphi + C_2 \cos\varphi + C_3 \sin\varphi. \quad (40)$$

In Eqs. (39), (40)

$$C_w = \frac{\omega^2 R}{2AE_0 e}\left(\frac{Q}{2} - r_c q\right), \quad C_\phi = \frac{\omega^2}{4AE_0 e}\left(Rq - \frac{Q}{2}\right), \quad (41)$$

and C_0, C_1, C_2 C_3 are the constants of integration. The combination of Eq. (38) with Eq. (39) gives the expression of the radial displacement

$$U(\varphi) = \frac{\omega^2 R}{2AE_0} q - \frac{C_w}{3} \cos 2\varphi - \frac{1}{2} r_c C_2 \varphi \cos\varphi - \frac{1}{2} r_c C_3 \varphi \sin\varphi + \alpha \cos\varphi + \beta \sin\varphi. \quad (42)$$

In (42) α and β are constants of integration. We introduce a new function which is a component of the circumferential displacement and it does not depend on the radial coordinate r

$$V(\varphi) = \frac{\mathrm{d}U}{\mathrm{d}\varphi} = \frac{2}{3} C_w \sin 2\varphi - \frac{1}{2} r_c C_2 (\cos\varphi - \varphi \sin\varphi) - \frac{1}{2} r_c C_3 (\sin\varphi + \varphi \cos\varphi) - \alpha \sin\varphi + \beta \cos\varphi. \quad (43)$$

The constants of integration C_0, C_1, C_2, C_3, α, β can be computed from the boundary conditions. Figure 3 enumerates some possible boundary conditions.

5 Examples

In the examples the next numerical data are used: $a = 0.025$ m, $c = 0.035$ m, $b = 0.055$ m, $t = 0.002$ m, $E_1 = 2{\times}10^{11}$ Pa, $E_2 = 8{\times}10^{10}$ Pa, $\rho_1 = 7000\ \frac{\mathrm{kg}}{\mathrm{m}^3}$, $\rho_2 = 4000\ \frac{\mathrm{kg}}{\mathrm{m}^3}$, $\omega = 10^4\ \frac{1}{\mathrm{s}}$. The end cross sections of the two-layer composite curved beam given by φ_1 and φ_2.

5.1 Rotating half circular two-layer beam with fixed ends

The curved beam with fixed ends is shown in Figure 4. In this case $\varphi_1 = 0$ and $\varphi_2 = \pi$ as it can be seen in Figure 4. The displacement functions $U = U(\varphi)$, $V = V(\varphi)$ and the cross-sectional rotations are given in Figures 5, 6 and 7. The normal force N, shear force S and bending moment M are plotted against the polar angle φ in Figures 8, 9 and 10. Figures 11 and 12 show the σ_φ as a function of r for seven different values of polar angle.

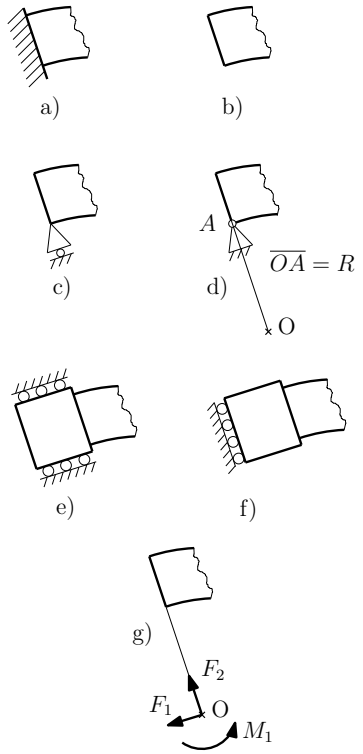

Figure 3: In-plane boundary conditions for two-layer composite beams: a) Fixed end: $U = 0$, $V = 0$, $\phi = 0$. b) Free end: $N = 0$, $S = 0$, $M = 0$. c) Simply supported end cross section in radial direction: $U = 0$, $M = 0$, $N = 0$. d) Pinned end: $U = 0$, $r_A\phi + V = 0$, $M - r_A N = 0$. e) Clamped circumferentially guided end: $U = 0$, $\phi = 0$, $N = 0$. f) Clamped radially guided end: $V = 0$, $\phi = 0$, $S = 0$. g) Loaded end cross section: $N = F_1$, $S = F_2$, $M = M_1$.

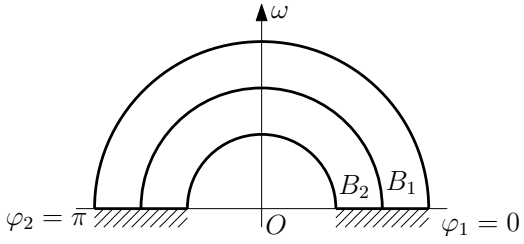

Figure 4: Rotating half circular two-layer beam.

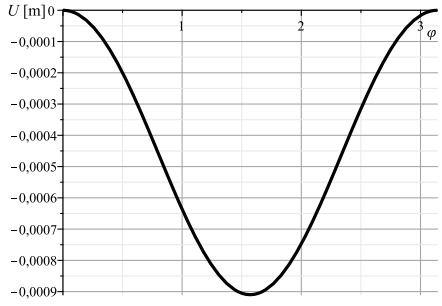

Figure 5: Plot of $U(\varphi)$ (Example 5.1).

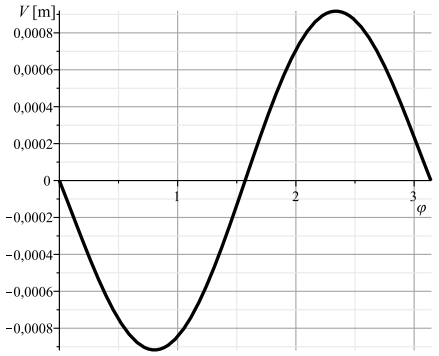

Figure 6: Plot of $V(\varphi)$ (Example 5.1).

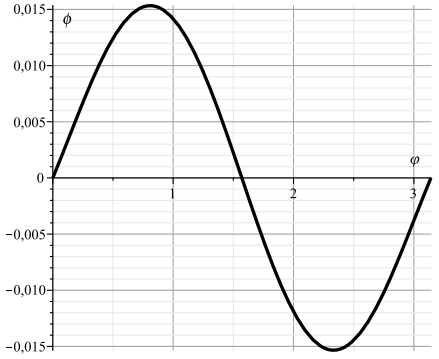

Figure 7: Plot of $\phi(\varphi)$ (Example 5.1).

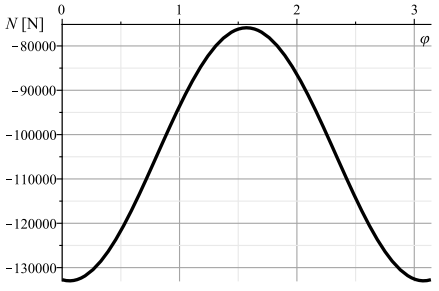

Figure 8: Plot of $N(\varphi)$ (Example 5.1).

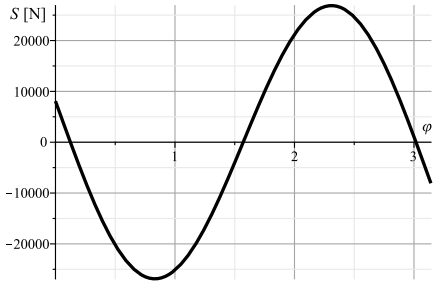

Figure 9: Plot of $S(\varphi)$ (Example 5.1).

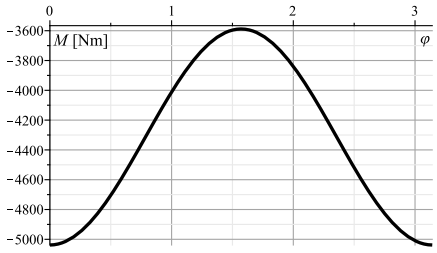

Figure 10: Plot of $M(\varphi)$ (Example 5.1).

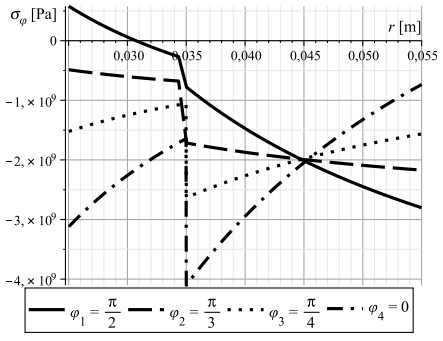

Figure 11: Plot of σ_φ as a function of r for φ_i $(i = 1 \ldots 4)$ (Example 5.1).

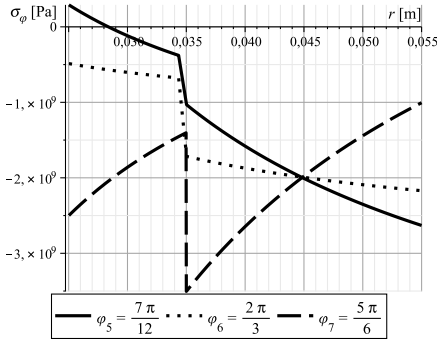

Figure 12: Plot of σ_φ as a function of r for φ_i $(i = 5 \ldots 7)$ (Example 5.1).

5.2 Rotating half circular beam with radially guided ends

The curved beam considered in Example 5.2 is shown in Figure 13. The displacement functions $U = U(\varphi)$, $V = V(\varphi)$ and cross-sectional rotation $\phi = \phi(\varphi)$ are illustrated in Figures 14, 15 and 16. The normal force N, shear force S and bending moment M are plotted against the polar angle φ in Figures 17, 18 and 19. Figures 20 and 21 show σ_φ as a function of r for seven different values of polar angle.

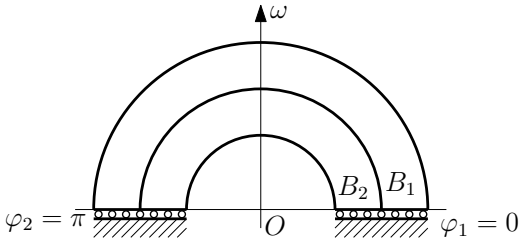

Figure 13: Rotating half circular beam with radially guided ends.

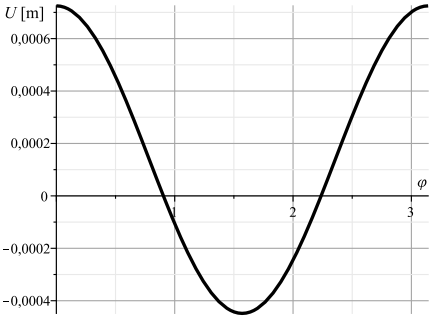

Figure 14: Plot of $U(\varphi)$ (Example 5.2).

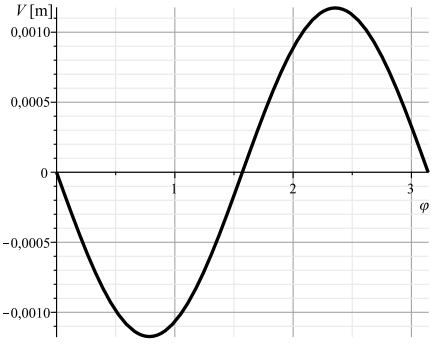

Figure 15: Plot of $V(\varphi)$ (Example 5.2).

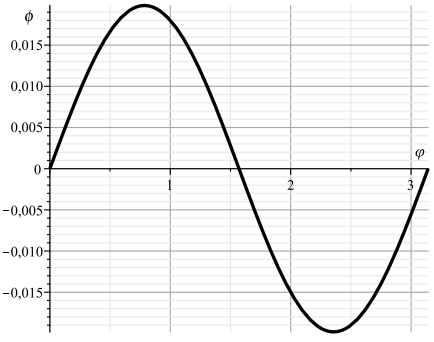

Figure 16: Plot of $\phi(\varphi)$ (Example 5.2).

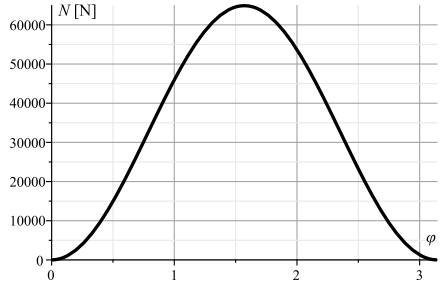

Figure 17: Plot of $N(\varphi)$ (Example 5.2).

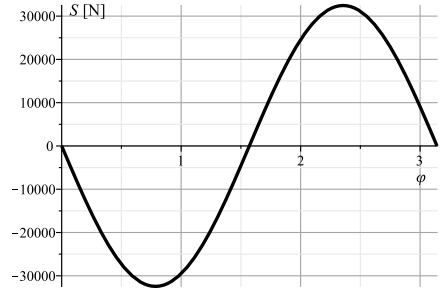

Figure 18: Plot of $S(\varphi)$ (Example 5.2).

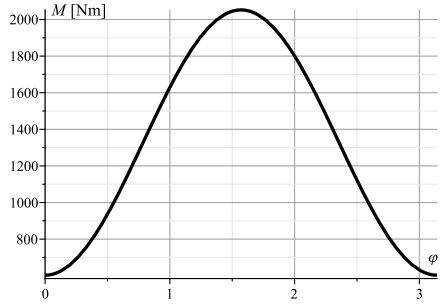

Figure 19: Plot of $M(\varphi)$ (Example 5.2).

5.3 Rotating of two-layer composite closed ring

The considered ring is illustrated in Figure 22. In this example $\varphi_1 = -\frac{\pi}{2}$, $\varphi_2 = \frac{3\pi}{2}$. The functions $U = U(\varphi)$, $V = V(\varphi)$ and $\phi = \phi(\varphi)$ are given in Figures 23, 24 and 25. The normal force N, shear force S and bending moment M are plotted against the polar angle φ in Figures 26, 27 and 28. Figures 29 and 30 illustrate the graphs of σ_φ as a function of r seven different value of φ.

5.4 Rotating two-layer composite split ring

In this example $\varphi_1 = -\frac{\pi}{2}$, $\varphi_2 = \frac{3\pi}{2}$ as shown in Figure 31. The displacement functions $U = U(\varphi)$, $V = V(\varphi)$ and cross-

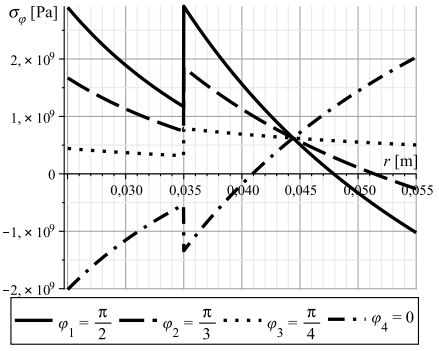

Figure 20: Plot of σ_φ as a function of r for φ_i $(i = 1 \ldots 4)$ (Example 5.2).

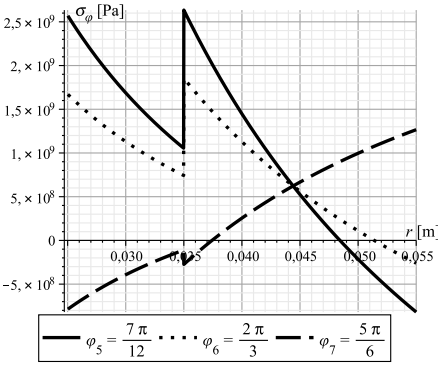

Figure 21: Plot of σ_φ as a function of r for φ_i $(i = 5 \ldots 7)$ (Example 5.2).

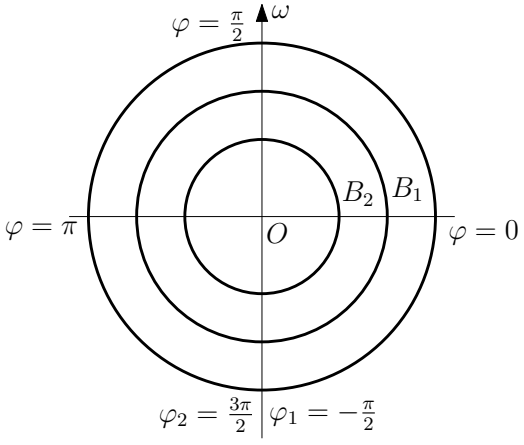

Figure 22: Rotating of two-layer composite closed ring.

sectional rotation function $\phi = \phi(\varphi)$ are shown in Figures 32, 33 and 34. The normal force N, shear force S and bending moment M as a function of φ are given in Figures 35, 36 and 37. Figures 38 and 39 provide the graphs of σ_φ as a function of r for seven different value of φ.

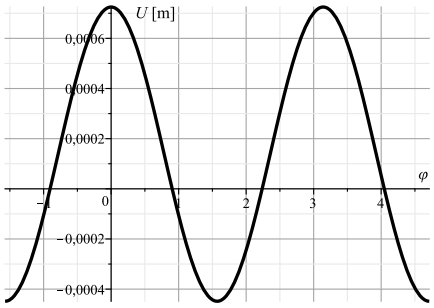

Figure 23: Plot of $U(\varphi)$ (Example 5.3).

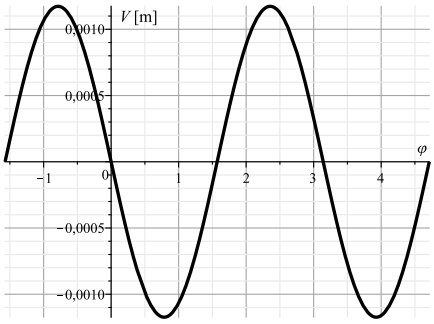

Figure 24: Plot of $V(\varphi)$ (Example 5.3).

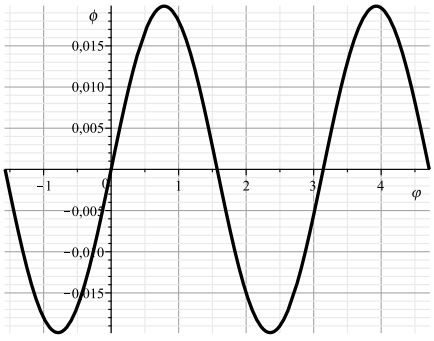

Figure 25: Plot of $\phi(\varphi)$ (Example 5.3).

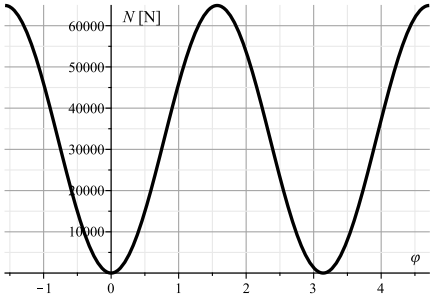

Figure 26: Plot of $N(\varphi)$ (Example 5.3).

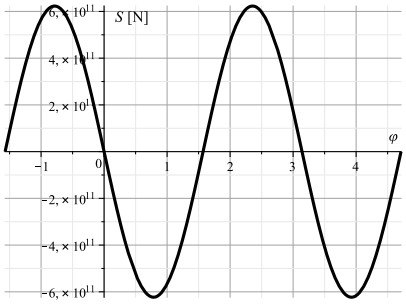

Figure 27: Plot of $S(\varphi)$ (Example 5.3).

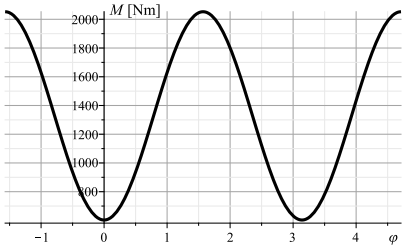

Figure 28: Plot of $M(\varphi)$ (Example 5.3).

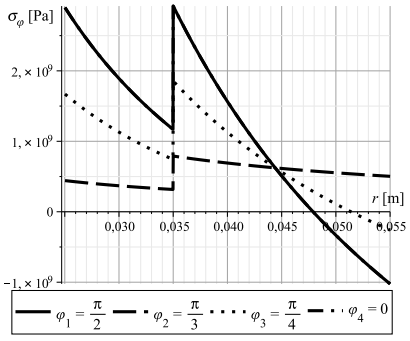

Figure 29: Plot of σ_φ as a function of r for φ_i $(i = 1 \ldots 4)$ (Example 5.3).

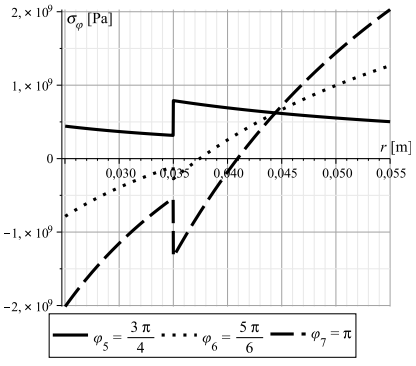

Figure 30: Plot of σ_φ as a function of r for φ_i $(i = 5 \ldots 7)$ (Example 5.3).

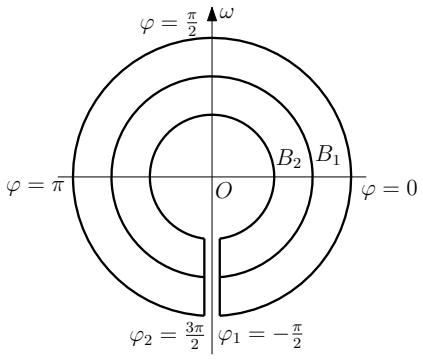

Figure 31: Rotating two-layer composite split ring.

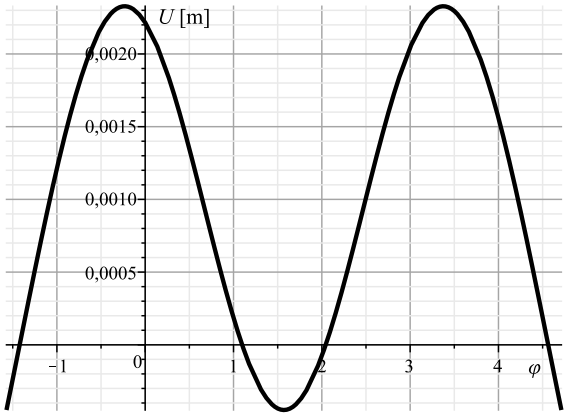

Figure 32: Plot of $U(\varphi)$ (Example 5.4).

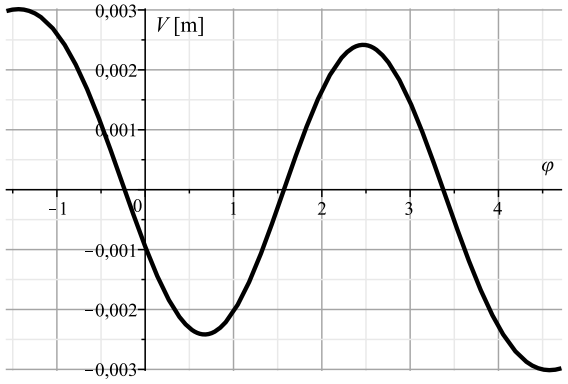

Figure 33: Plot of $V(\varphi)$ (Example 5.4).

6 Supplementary comment: Multilayered curved beam

Although the paper gives the detailed derivation of governing equations for two-layer composite beam the results of Sections 3–5 can be extended for multilayered curved composite beam (Figure 40). All equations of Sections 2–5 can be used if we redefine the cross sectional properties according to the next equations

$$A_i = t(a_{i+1} - a_i), \quad A = t(a_{n-1} - a_1), \tag{44}$$

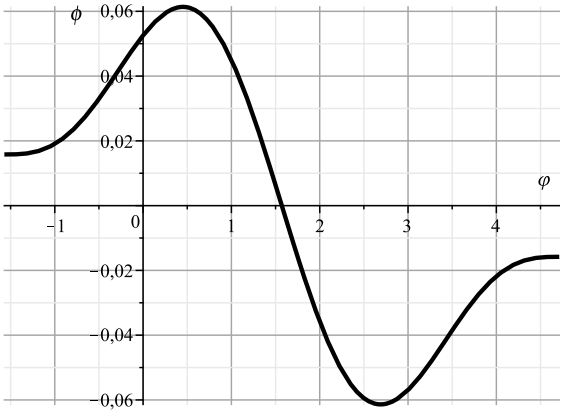

Figure 34: Plot of $\phi(\varphi)$ (Example 5.4).

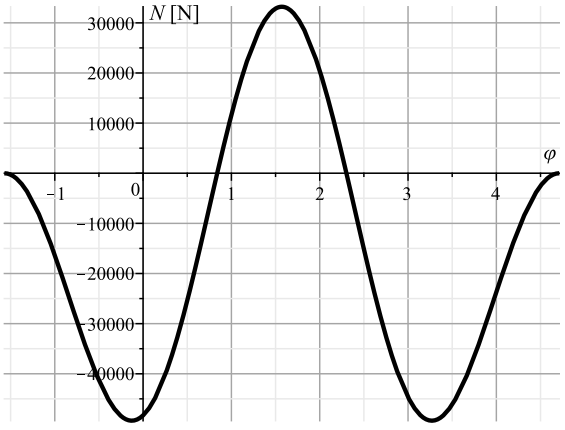

Figure 35: Plot of $N(\varphi)$ (Example 5.4).

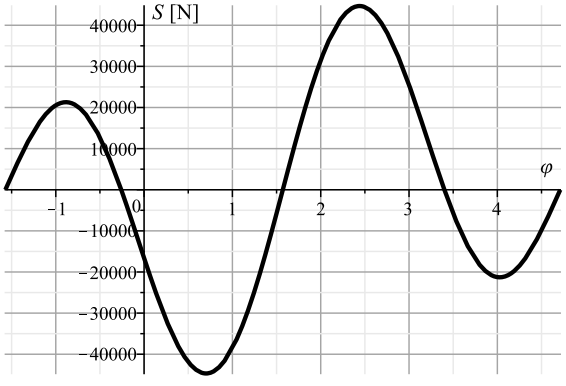

Figure 36: Plot of $S(\varphi)$ (Example 5.4).

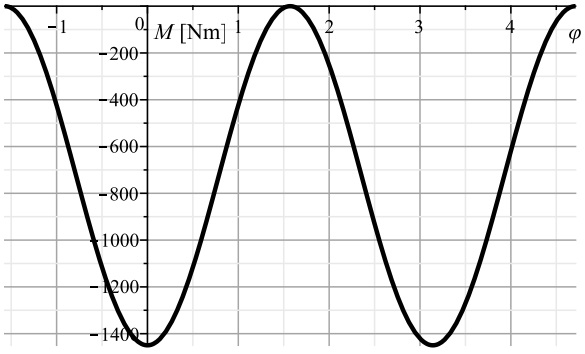

Figure 37: Plot of $M(\varphi)$ (Example 5.4).

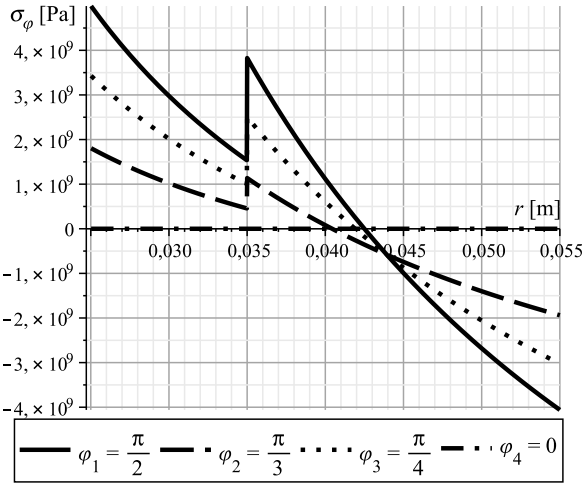

Figure 38: Plot of σ_φ as a function of r for φ_i ($i = 1 \ldots 4$) (Example 5.4).

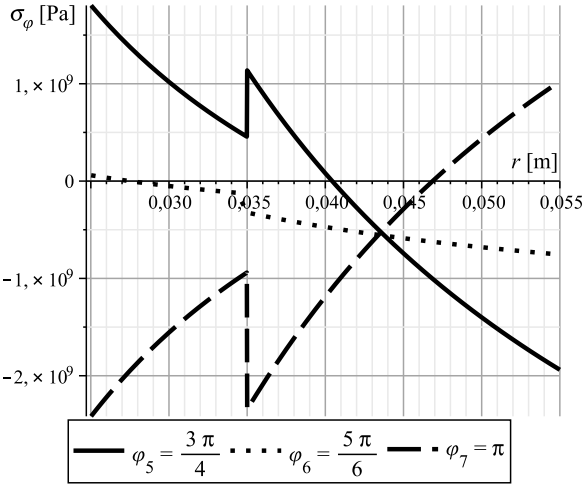

Figure 39: σ_φ as a function of r for φ_i ($i = 5 \ldots 7$) (Example 5.4).

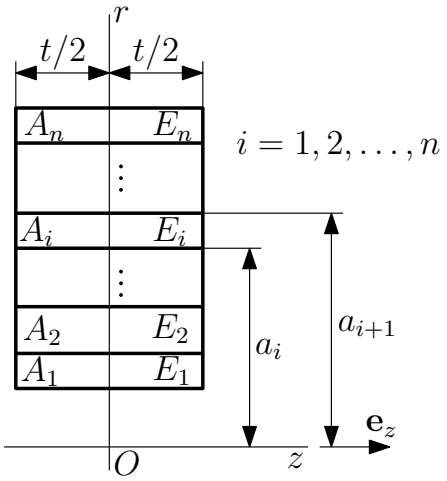

Figure 40: Cross section of multilayered composite beam.

$$E_0 = \frac{\sum_{i=1}^{n}(a_{i+1} - a_i)E_i}{a_{n+1} - a_i}, \tag{45}$$

$$r_c = \frac{\sum_{i=1}^{n} E_i\left(a_{i+1}^2 - a_i^2\right)}{2(a_{n+1} - a_i)E_0}, \tag{46}$$

$$R = \frac{a_{n+1} - a_1}{\sum_{i=1}^{n} \frac{E_i}{E_0} \ln \frac{a_{i+1}}{a_i}}, \quad e = r_c - R, \tag{47}$$

$$q = t\sum_{i=1}^{n-1} \rho_i \frac{a_{i+1}^3 - a_i^3}{3}, \tag{48}$$

$$Q = t\sum_{i=1}^{n-1} \rho_i \frac{a_{i+1}^4 - a_i^4}{4}. \tag{49}$$

Introducing this cross-sectional properties into the formula (40) and (42) we can directly obtain the cross-sectional rotation and the radial displacement fields for multilayered beam. It is evident that the formula of normal stress $\sigma_\varphi = \sigma_\varphi(r, \varphi)$ can be represented as

$$\sigma_\varphi(r, \varphi) = \sum_{i=1}^{n} E_i \left[H(r - a_i) - H(r - a_{i+1})\right] \left[\frac{1}{r}\left(U + \frac{\mathrm{d}^2 U}{\mathrm{d}\varphi^2}\right) + \frac{\mathrm{d}\phi}{\mathrm{d}\varphi}\right]. \tag{50}$$

In Eq. (50)

$$H(r - a) = \begin{cases} 0, & r \le 0, \\ 1, & r > 0 \end{cases} \tag{51}$$

is the Heaviside function.

7 Conclusions

Paper gives an analytical solution to obtain the deformation a rotating curved two-layer circular composite beam. The formulation and solution of the considered equilibrium problem of rotating curved beam is based on the Euler-Bernoulli beam theory. The rotary inertia is included in the system of centrifugal forces. The numerical examples of this paper can be used as benchmark solutions to check the validity of solutions obtained by other methods such as finite element method, finite difference method, etc.

Acknowledgement: The described study was carried out as a part of the EFOP-3.6.1-16-2016-00011 "Younger and Renewing University – Innovative Knowledge City – institutional development of the University of Miskolc aiming at intelligent specialisation" project implemented in the framework of the Szechenyi 2020 program. The realization of this project is supported by the European Union, co-financed by the European Social Fund and supported by the National Research, Development and Innovation Office - NKFIH, K115701.

References

[1] Segura J.M., Armengaud G., Analytical formulation of stresses in curved composite beams, Archive of Applied Mechanics, 1998, 68(3-4), 206-213., DOI: https://dx.doi.org/10.1007/s004190050158

[2] Wang M., Liu Y., Elasticity solutions for orthotropic functionally graded curved beams, European Journal of Mechanics - A/Solids, 2013, 37, 8-16., DOI: https://dx.doi.org/10.1016/j.euromechsol.2012.04.005

[3] Pydah A., Sabale A., Static analysis of bi-directional functionally graded curved beams, Composite Structures, 2017, 160, 867-876., DOI: https://dx.doi.org/10.1016/j.compstruct.2016.10.120

[4] Ecsedi I., Lengyel A.J., Curved composite beam with interlayer slip loaded by radial load, Curved and Layered Structures, 2015, 2(1), 50-58., DOI: https://dx.doi.org/10.1515/cls-2015-0004

[5] Ecsedi I., Lengyel A.J., Energy methods for curved composite beams with partial shear interaction, Curved and Layered Structures, 2015, 2(1), 351-361., DOI: https://dx.doi.org/10.1515/cls-2015-0020

[6] Ecsedi I., Lengyel A.J., An analytical solution for static problems of curved composite beams, Curved and Layered Structures, 2019, 6(1), 105-116., DOI: https://dx.doi.org/10.1515/cls-2019-0009

[7] Ibrahimbegović A., Frey F., Finite element analysis of linear and non-linear planar deformations of elastic initially curved beams, International Journal for Numerical Methods in Engineering, 1993, 36(19), 3239-3258., DOI: https://dx.doi.org/10.1002/nme.1620361903

[8] Ascione L., Fraternali F., A penalty model for the analysis of curved composite beams, Computers and Structures, 1992, 45(5-6), 985-999., DOI: https://dx.doi.org/10.1016/0045-7949(92)90057-7

[9] Bhimaraddi A., Carr A.J., Moss P.J., Generalized finite element analysis of laminated curved beams with constant curvature, Computers and Structures, 1989, 31(3), 309-317., DOI: https://dx.doi.org/10.1016/0045-7949(89)90378-7

[10] Dorfi H.R., Busby H.R., An effective curved composite beam finite element based on the hybrid-mixed formulation, Computers and Structures, 1994, 53(1), 43-52., DOI: https://dx.doi.org/10.1016/0045-7949(94)90128-7

[11] Kim J.-G., An effective composite laminated curved beam element, Communications in Numerical Methods in Engineering, 2006, 22(5), 453-466., DOI: https://dx.doi.org/10.1002/cnm.829

[12] Ecsedi I., Dluhi K., A linear model for the static and dynamic analysis of non-homogeneous curved beams, Applied Mathematical Modelling, 2005, 29(12), 1211-1231., DOI: https://dx.doi.org/10.1016/j.apm.2005.03.006

[13] Wang J.T.S., Mahrenholtz O., Bending frequencies of a rotating curved beam, Ingenieur-Archiv, 1975, 44(6), 399-407., DOI: https://dx.doi.org/10.1007/BF00534621

[14] Park J.-H., Kim J.-H., Dynamic analysis of rotating curved beam with a tip mass, Journal of Sound and Vibration, 1999, 228(5), 1017-1034., DOI: https://dx.doi.org/10.1006/jsvi.1999.2457

[15] Chen Y., Zhang D., Li L., Dynamic analysis of rotating curved beams by using Absolute Nodal Coordinate Formulation based on radial point interpolation method, Journal of Sound and Vibration, 2019, 441, 63-83., DOI: https://dx.doi.org/10.1016/j.jsv.2018.10.011

[16] Chidamparam P., Leissa A.W., Vibrations of planar curved beams, rings, and arches, Applied Mechanics Reviews, 1993, 46(9), 467-483., DOI: https://dx.doi.org/10.1115/1.3120374

[17] Kartav O., Vibration analysis of rotating curved beams with variable cross-section, Thesis, 2014, Department of Mechanical Engineering, Izmir Institute of Technology